Effect of transition metal ions on the fluorescence and Taq-catalyzed polymerase chain reaction of tricyclic cytidine analogs

ARTICLE *in* ANALYTICAL BIOCHEMISTRY · APRIL 2011

Impact Factor: 2.22 · DOI: 10.1016/j.ab.2011.04.033 · Source: PubMed

3 AUTHORS, INCLUDING:

Robert Kuchta
University of Colorado at Boulder
91 PUBLICATIONS **2,592** CITATIONS

SEE PROFILE

Published in final edited form as:
Anal Biochem. 2011 September 1; 416(1): 53–60. doi:10.1016/j.ab.2011.04.033.

Effect of transition metal ions on the fluorescence and Taqcatalyzed PCR of tricyclic cytidine analogues

Gudrun Stengel[1], **Byron Purse**[2], and **Robert D. Kuchta**[1,*]

[1]Department of Chemistry and Biochemistry, University of Colorado, Boulder, CO 80309-0215

[2]Department of Chemistry and Biochemistry, University of Denver, Denver, Colorado 80208

Abstract

The cytosine analogues 1,3-diaza-2-oxophenothiazine (tC) and 1,3-diaza-2-oxophenoxazine (tCo) stand out among fluorescent bases due to their unquenched fluorescence emission in double-stranded DNA. Recently, we reported a method for the generation of densely tCo-labeled DNA by polymerase chain reaction (PCR) that relied on the use of the extremely thermostable Deep Vent polymerase. We have now developed a protocol that employs the more commonly used Taq polymerase. Supplementing the PCR with Mn^{2+} or Co^{2+} ions dramatically increased the amount of dtCoTP incorporated, and thus enhanced the brightness of the PCR products. The resulting PCR products could be easily detected in gels based on their intrinsic fluorescence. The Mn^{2+} ions modulate the PCR by improving the bypass of template tCo and the overall catalytic efficiency. In contrast to the lower fidelity during tCo bypass, Mn^{2+} improved the ability of Taq polymerase to distinguish between dtCoTP and dTTP when copying a template dA. Interestingly, Mn^{2+} ions hardly affect the fluorescence emission of tC(o), whereas the coordination of Co^{2+} ions with the phosphate groups of DNA and nucleotides statically quenches tC(o) fluorescence with small reciprocal Stern Vollmer constants of 10 to 300 μM.

Keywords

polymerase chain reaction; fluorescence; quenching; taq; manganese; cobalt; kinetics

INTRODUCTION

Fluorescent base analogues play an important role as probes in today's life sciences owing to the sensitivity of their fluorescent properties to the polarity of their microenvironment[1]. Sensitive and affordable optical instrumentation allows measuring changes in fluorescence intensity, polarization, and lifetime, parameters that provide valuable insights into the nature of molecular interactions and the structural dynamics of nucleic acid complexes. Base analogues are widely employed to observe structural rearrangements in nucleic acids, such as hybridization/melting[2-6], loop formation and base flipping [7, 8], and they have helped to elucidate the catalytic mechanism of many DNA modifying enzymes[7, 9-11]. In biotechnology, base analogues are established building blocks of hybridization probes that are used to screen for specific DNA sequences, single nucleotide polymorphisms and DNA groove binders[12, 13].

Although many fluorescent base analogues have been reported, there is still a shortage of analogues that can be enzymatically incorporated into long nucleic acids, and which remain

*Address correspondence to this author: kuchta@colorado.edu, Phone: 303-492-7027.

intensely fluorescent upon incorporation into DNA. The cytosine analogues 1,3-diaza-2-oxophenothiazine (tC) and 1,3-diaza-2-oxophenoxazine (tCo) meet both of these criteria: they are nearly impervious to quenching in single and double-stranded DNA [14-16], and their triphosphates are excellent DNA and RNA polymerase substrates that are incorporated with high catalytic efficiency and moderate specificity by a large number of polymerases [17, 18]. This characteristic allows their use as probes for the visualization of nucleic acids in analytical gels [18, 19]. Due to their resistance to quenching, tC and tCo hold great promise as probes for tracking the pathway of fluorescent nucleic acids injected into life cells and for measuring minute distance changes in biological assemblies using fluorescence resonant energy transfer (FRET) [20, 21].

Recently, we reported a PCR protocol for the synthesis of densely tCo-labeled DNA fragments (560 bp with 50 % of cytosine substituted for tCo) [18]. The PCR was contingent on the use of Deep Vent polymerase, an extremely thermostable B family polymerase, and repeated DNA denaturation at high temperatures (99°C). The commonly used Taq polymerase, a member of the A family, performed poorly under the same conditions, partly due to a shorter half life at elevated temperatures, but primarily due to differences in substrate specificity. These studies revealed that Taq polymerase discriminates less well against tCo-A base pairs than Deep Vent polymerase, and the resulting tCo-A base pairs constitute lesions that are not readily extended. As a consequence thereof, we observed chain termination at relatively low concentrations of tCo triphosphate (dtCoTP)[18].

While it is difficult to improve the substrate specificity of a polymerase through changes to the reaction conditions, some bivalent metal ions are known to enhance the catalytic efficiency of polymerases at the expense of fidelity [22-25]. Polymerases catalyze the addition of a nucleoside monophosphate to the 3’ terminus of a DNA primer via a substitution reaction: the 3’OH of 2’-deoxyribose attacks the α-phosphorus of the incoming nucleotide to form a phosphodiester linkage, with concomitant release of pyrophosphate [26-28]. In addition to catalytic amino acids, this mechanism requires two Mg^{2+} ions [29]. Metal A is thought to facilitate the deprotonation of the 3’OH moiety, and metal B coordinates the triphosphate of the incoming nucleotide, supporting nucleotide binding and pyrophosphate release [29, 30]. Kinetic studies, X-ray structures and quantum mechanical calculations show that not only Mg^{2+} but also Mn^{2+} ions can act as nucleophile activators [28, 31]. Owing to the different orbital structure and larger polarizability, Mn^{2+} ions dictate a less stringent alignment of the involved atoms, which results in facilitated, yet less selective nucleotidyl transfer. To date, improved bypass of damaged template bases, sugar and base analogues in the presence of Mn^{2+} has been reported across different families of DNA polymerases [24, 25, 32-36], raising the possibility that the trace element Mn^{2+} may even play a physiological role in translesion DNA synthesis [37].

Expanding on this idea, we show that supplementing the Mg^{2+}-containing reaction buffer with Mn^{2+} and Co^{2+} ions improves the bypass of template tCo by Taq polymerase, and we present optimized PCR protocols for the synthesis of tCo-labeled DNA using this more abundant, less expensive polymerase. In addition, we identify Co^{2+} as the first known quencher of tC(o) fluorescence and derive its quenching mechanism.

EXPERIMENTAL SECTION

Materials and Enzymes

Unlabeled dNTPs and Taq polymerase were from Invitrogen, ^{32}P-labeled NTPs from Perkin Elmer Life Sciences. Analytical grade $MnCl_2$ and $CoCl_2$ were obtained from Sigma Aldrich. The 1,3-diaza-2-oxophenothiazine and 1,3-diaza-2-oxo-phenoxazine nucleosides were synthesized according to Matteucci et al.[15] and converted into the 5’-triphosphate following

the procedure of Ludwig[38]. The concentration of tC and tCo containing molecules was determined based on their extinction coefficients at the wavelength of maximal absorbance ($\varepsilon_{tCo,\ 360\ nm}$ = 9,000 $M^{-1}cm^{-1}$; $\varepsilon_{tC,\ 375\ nm}$ = 4,000 $M^{-1}cm^{-1}$). The tC(o)-labeled oligonucleotides were synthesized in house, whereas unmodified oligonucleotides were purchased from Integrated DNA Technology. The plasmid coding for the globin protein was a gift from Jens Lyke-Andersen (University of Colorado Boulder).

PCR reactions and analysis

The 560 bp DNA fragment coding for the beta chain of human hemoglobin was amplified using 5'GTACGGTGGGAGGTCTATAT 3' (forward primer) and 5'ACCACTTTCTGATAGGCAGC 3' (reverse primer). The reactions (50 μL) contained 20 mM Tris-HCl pH 8.4, 50 mM KCl, 3.5 mM $MgCl_2$, the indicated concentration- of $MnCl_2$ or $CoCl_2$, 200 μM of dTTP, dATP and dGTP, varying amounts of dCTP and dtCoTP, 500 nM forward and reverse primer, 9.4 ng μL^{-1} template and 2.5 units Taq polymerase. The temperature program for reactions without betaine was: 30 cycles at 94°C/45 s; 55°C/30 s; 72°C/2 min 30 s; final elongation 72°C/10 min. The program for reactions with 1 M betaine was: 30 cycles at 97°C/20 s; 55°C/30 s; 72°C/2 min 30 s; final elongation 72°C/10 min. PCR amplification was performed in a Eppendorf Mastercycler. The PCR reactions were analyzed using 1.2 % agarose gels with 0.5 × TAE buffer. The gels were exposed either at 365 nm to detect DNA directly via tCo fluorescence or at 254 nm after staining of the DNA bands with ethidium bromide.

5'-labeling of primer strands

DNA primers were 5'-^{32}P-labeled using T4 polynucleotide kinase (New England Biolabs) and [γ-^{32}P]ATP. The labeled primer was gel-purified and annealed to the appropriate template strands.

Polymerization assays

Each reaction (10 μL) contained 20 mM Tris-HCl pH 8.4, 50 mM KCl, 0.5 mM $MnCl_2$, 3 mM $MgCl_2$, 0.05 mg/ml bovine serum albumin, 0.5 μM 5'-^{32}P-primer/template and between 0.1 and 200 μM of the nucleotide of interest. In assays that probed the incorporation at the +3 position across from T, the nucleotides complementary to the +1 and +2 template positions were included at a constant concentration of 100 μM each, and the dATP concentration was varied. The base sequences of the primer/templates were as follows:

DNA_A

5′–TCC ATA TCA CAT

3′–AGG TAT AGT GTA **A** CTC TTA TCT ATC T

DNA_T

5′–TCC ATA TCA CAT

3′–AGG TAT AGT GTA **T** CTC TTA TCT ATC T

DNA_G

5′–TCC ATA TCA CAT

3′–AGG TAT AGT GTA **G** CTC TTA TCT ATC T

DNA_C

5′–TCC ATA TCA CAT

3′–AGG TAT AGT GTA **C** ATC TTA TCT ATC T

DNA_{tCo}

5′–TCC ATA TCA CAT

3′–AGG TAT AGT GTA **tCo** ATC TTA TCT ATC T

Polymerization was initiated by addition of Taq pol to a final concentration of 0.01 units/μL, followed by incubation at 37 °C. Two volumes gel loading buffer (90 % formamide with 50 mM EDTA) were added to stop the reactions. The extension products were separated by denaturing gel electrophoresis (20% polyacrylamide, 8 M urea) and analyzed by phosphor imaging (Typhoon scanner, Molecular Dynamics). The parameters V_{max} and K_M were obtained by plotting primer extension as a function of dNTP concentration and subsequent non-linear curve fitting of the data to the Michaelis-Menten equation.

Competitive single nucleotide extension assays

To measure the competitive insertion of dCTP and dtCoTP across from G, assays contained DNA_G and 20 μM dNTP total. Eight reactions were set up with different mixing ratios of the competing dNTPs. The concentration of Taq pol was 0.01 units/μL, and the reactions were stopped after 5 and 10 minutes. The reaction products were separated on a 20 % polyacrylamide, 8 M urea gel and the fraction of primer that had been extended by tCo or by C was quantified. The relative kcat/K_M values were determined graphically using the following equation: $$\frac{1}{fraction_{dNTP}} = \frac{\left(\frac{kcat}{K_M}\right)_{dtCoTP}}{\left(\frac{kcat}{K_M}\right)_{dNTP}} \cdot \frac{[dtCoTP]}{[dCTP]}$$, with $fraction_{dNTP}$ being the amount of primer extended by C in this case[39]. Analogous experiments were performed with DNA_A and mixtures of dtCoTP and dTTP. The resulting reaction products required separation on a 25% polyacrylamide, 8 M urea gel.

Fluorescence quenching

Emission spectra were recorded using the Quantamaster steady-state fluorimeter from Photon Technology International. All slits were set to 1 nm, the excitation wavelength was 360 nm for tCo and 380 nm for tC, respectively. All samples (130 μL total) contained 0.5 μM of the analogue labeled molecules in 20 mM Tris pH 8 and 50 mM NaCl. Fluorescence spectra were recorded prior and after addition of each concentration of quencher; in each case, the quencher had no effect on the shape of the spectra. The obtained intensities were corrected for dilution of the sample by the added volume of quencher. The quenching data were analyzed using the Stern Vollmer equation, $F_0/F=1+K_{SV}[Q]$. Fo and F are the fluorescence intensities in the absence and presence of the quencher Q, and K_{SV} is the Stern Vollmer constant, and [Q] is the quencher concentration.

RESULTS AND DISCUSSION

Improvement of PCR using Mn^{2+} and Co^{2+} ions

We previously found that Taq polymerase does not effectively incorporate tCo into DNA during PCR reactions [18]. To explore if Mn^{2+} ions can relieve the replication block that prevents Taq polymerase from replacing more than 5 % of cytosine with the analogue tCo [18], we PCR amplified a 560 bp fragment of the human hemoglobin gene at varying Mn^{2+} concentrations. We also tested Co^{2+} in analogous reactions since it also reduces the fidelity of some DNA polymerases [40]. Additionally, Co^{2+} can quench the fluorescence of various fluors [41-46].

The agarose gel in Figure 1 shows the DNA bands obtained in two sets of standard PCR reactions with denaturation at 94 °C. The reactions on the left contained only natural dNTPs, each at 200 μM, and either Mg^{2+} alone (3.5 mM), or Mg^{2+} supplemented with increasing amounts of Mn^{2+} or Co^{2+} (0.2; 0.5; 1 mM). The PCR functioned optimally with Mg^{2+} alone and adding different metal ions inhibited the reactions. The reactions on the right were analogous, with the important difference that they contained 175 μM dCTP and 25 μM dtCoTP. Here, no product was obtained with Mg^{2+} alone, and optimal performance was achieved either 0.5 mM Mn^{2+} or Co^{2+}, respectively. Thus, the presence of these alternate cofactors allowed the synthesis of DNA at dtCoTP concentrations where the PCR with Mg^{2+} failed.

To test the limits of dtCoTP incorporation, we fixed the metal ion concentrations at 3.5 mM Mg^{2+} plus either 0.5mM Mn^{2+} or Co^{2+}, and varied the dtCoTP concentration from 10 to 40 μM (Figure 2A). We observed intrinsically fluorescent DNA bands up to 30 μM dtCoTP, even though the total amount of amplified DNA decreased. However, no detectable product was formed at 40 μM dtCoTP. Since the higher dtCoTP concentration presumably results in greater dtCo incorporation, these data suggest that even Mn^{2+} or Co^{2+} do not allow efficient replication of templates containing a high density of tCo.

As discussed previously, the presence of tCo in PCR products increases the melting temperature of DNA, which necessitated a harsh denaturation step at 99°C in the presence of 15 % glycerol for optimal PCR with Vent polymerase [18]. However, Taq polymerase will not tolerate as high temperatures as Deep Vent polymerase, even in the presence of stabilizing glycerol. We repeated the reactions described in Figure 2A using glycerol, DMSO or betaine, reagents commonly used to facilitate the amplification of GC rich amplicons [47-50]. None of these reagents was shown to generally outperform the others in typical PCR applications, but their utility depends on the individual base sequence [47, 48]. In our case, optimal results were obtained using a denaturation step at 97°C (20s) in the presence of 1M betaine (Figure 2 B, bottom). These reaction conditions permitted significantly improved detection of the unstained PCR products based on their intrinsic tCo fluorescence (Figure 2B, top) up to a dtCoTP concentration of 50 μM (not shown). To our surprise, betaine alone allowed for tCo incorporation, without the requirement for transition metal ions.

In light of previous studies showing that Mn^{2+} and Co^{2+} compromise the fidelity of DNA polymerases [22, 23, 25, 40], the products of these PCR reactions will likely contain more mutations than the products of PCR reactions that contain only Mg^{2+}. Furthermore, tCo incorporation itself will result in mutations in the product because DNA polymerases have only a moderate ability to discriminate against dtCoTP incorporation opposite A and dATP incorporation opposite dtCo. Nonetheless, the mutation rate is sufficiently low to ensure primer hybridization in each PCR cycle. In most cases, practitioners of PCR prefer to carry out DNA amplification in an accurate manner; however, there are instances where base insertion promiscuity is irrelevant or even desired. Mutagenic PCR is oftentimes used to deliberately randomize stretches of a gene. The resulting library of proteins or nucleic acids is screened for a particular property in order to gain insight into important structure-function relationships. Amplification accuracy is also secondary when pursuing analytical objectives: one may want to control the success of a ligation reaction or of the insertion of a point mutation or restriction site, or simply demonstrate the concept of PCR in an educational setting. In these instances, tCo labeling enables the detection of DNA without producing toxic waste, perhaps making the teaching of PCR concepts more amenable to less academic settings, such as high schools.

Comparison of the kinetics of Mg^{2+} and Mn^{2+}-catalyzed polymerization reactions

Our PCR data above show that both Mn^{2+} and Co^{2+} ions increase the amount of dtCoTP that Taq polymerase incorporates into DNA. For better quantification and to deepen our understanding of the mechanism by which Mn^{2+} and Co^{2+} ions affect DNA polymerization, we refocused our study on short, synthetic 5'[^{32}P]-labeled primer/templates (see experimental section) to determine how Mn^{2+} allows PCR in the presence of dtCoTP.

To capture general trends, we performed polymerization assays that were designed to produce a single tCo-G base pair and otherwise fully matched 26 bp DNA. To test the effect of metal ions on dNTP polymerization following dtCoTP insertion, DNA_G (see experimental section) was extended in the presence of dATP, dTTP, dGTP and dtCoTP. The effect of a templating tCo was studied by extension of DNA_{tCo} in the presence of all four natural dNTPs (Figure 3). We supplemented the reaction buffer (3 mM $MgCl_2$) with increasing amounts of either $MnCl_2$ or $CoCl_2$ (to 0.1; 0.2, or 0.5 mM) and quantified the amount of total primer extension, as well as the percentage of primer extended beyond the +3 template position. Increasing the Mn^{2+} and Co^{2+} concentration reduced pausing of Taq polymerase at the +2 and +3 template positions and improved the bypass and extension of the tCo containing base pair (Figure 3, table 1). Despite improved read-through, the amount of fully extended DNA only increased when DNA_{tCo} was the template because for DNA_G, the addition of Mn^{2+} and Co^{2+} led to inhibition of the overall primer extension (table 1). The inhibition was slightly more pronounced in the reactions containing Co^{2+} ions.

To determine if Mn^{2+} and Co^{2+} gave different levels of misincorporation, we measured both single nucleotide insertion opposite a template tCo (Figure 4 left) and incorporation of dtCoTP across from the four natural bases (Figure 4 right). In some cases the transition metal ions caused significantly higher misinsertion. Since the effects were particularly pronounced for Mn^{2+} ions, we decided to limit the following detailed kinetic study to Mn^{2+} ions and the most prominent mismatch, tCo-A and A-tCo.

Previous attempts to incorporate a moderate amount of dtCoTP by Taq polymerase in Mg^{2+}-catalyzed PCR reactions failed due to a lack of discrimination against dATP across from a template tCo combined with the inability to efficiently extend the resulting base mismatch [18]. To find out how the mismatch frequency changes in the presence of Mn^{2+}, we measured V_{max} and K_M for single nucleotide insertions by Taq polymerase using synthetic primer/templates (table 2). Three observations are noteworthy: First, compared to identical Mg^{2+}-catalyzed reactions, the presence of Mn^{2+} ions increased the overall efficiency of the insertion of both dGTP and dATP opposite a template tCo or C, respectively. The relative catalytic efficiency for the formation of the identical base pair in the presence of different catalytic ions $(V_{max}/K_M)_{Mn2+}/(V_{max}/K_M)_{Mg2+}$ is moderately high and ranges between 2 and 7. Mn^{2+} dramatically facilitates the incorporation of dATP across from C $((V_{max}/K_M)_{Mn2+}/(V_{max}/K_M)_{Mg2+} = 2000)$. Second, the efficiency of the bypass of dA-tCo and dA-C base pairs is improved 10- and 13-fold, respectively, in the presence of Mn^{2+}, as measured by the efficiency of the incorporation of the succeeding correct nucleotide at the +2 position. We did not examine the extension of the correct dG-tCo base pair because it was not found to be problematic[17]. Taken together, the discrimination against dATP-tCo mismatches $[(V_{max}/K_M)_{dGTP\text{-}tCo}/(V_{max}/K_M)_{dATP\text{-}tCo}]_{\mathbf{Mn2+}} = 12$ is poorer than with Mg^{2+} $[(V_{max}/K_M)_{dGTP\text{-}tCo}/(V_{max}/K_M)_{dATP\text{-}tCo}]_{\mathbf{Mg2+}} = 27$ but the resulting dA-tCo mismatch is much more readily extended. Third and rather surprisingly, when dtCoTP is the incoming nucleotide that competes with dCTP or dTTP, respectively, for incorporation opposite a template G or A, respectively, dtCoTP is less likely to win the competition in the presence of Mn^{2+} ions. Thus, fewer dtCoTP-A mismatches are generated with Mn^{2+} than with Mg^{2+} alone.

Although these single nucleotide incorporation studies are limited to a particular base context, they point out at least two factors that likely contribute to the success of the PCR in the presence of Mn^{2+}: reduced generation of dtCoTP-dA mismatches and improved extension of any dtCo-dA mismatches that do form. Substitution of Mg^{2+} with Mn^{2+} ions has been reported to confer the bypass or incorporation of other non-canonical nucleotides by members of all DNA polymerase families: e. g. O6-methyl-guanine by Klenow fragment and DNA polymerase alpha [36], C-8 guanyl-2-aminofluorene by Klenow fragment and T7 DNA polymerase [24], intrastrand cis-platin adducts by herpes simplex virus DNA polymerase [35], thymine dimers and N-ethyl-guanine by DNA polymerase iota [34], and 2-aminopurine nucleotide incorporation and bypass of abasic sites by T4 DNA polymerase [33]. While manganese-induced lesion bypass is a relatively common phenomenon that is typically associated with a general loss of fidelity, the 10-fold enhanced discrimination against dtCoTP-A base pairs is unusual. A possible, although unproven explanation would be that the relaxed alignment of active site residues caused by Mn^{2+} also destabilizes the imino tautomer of dtCoTP, which is an electronic isostere of T. To our knowledge, enhanced mismatch discrimination in the presence of Mn^{2+} has only been reported for DNA polymerase iota, which exhibits improved substrate selectivity across a template T in the presence of Mn^{2+} [32].

Quenching of tC(o) fluorescence by Mn^{2+} and Co^{2+}

As demonstrated above, Mn^{2+} and Co^{2+} ions can both substitute for the natural cofactor Mg^{2+} in polymerase reactions. Since transition metal ions are common quenchers of fluorescence, these ions may offer the possibility to modulate the emission of the tC(o) base as a function of its chemical environment, which would be of interest for various biotechnological applications.

Initial quenching experiments revealed that Co^{2+} ions quench the fluorescence of tCo labeled nucleic acids and nucleotides profoundly, whereas Mg^{2+} and Mn^{2+} ions were poor quenchers of tCo fluorescence. The quenching data were analyzed using the Stern Vollmer equation, $F_0/F=1+K_{SV}[Q]$ [51]. For single and double-stranded tCo-containing DNA, the quenching efficiency increased nearly linearly with the Co^{2+} concentration in accordance with the Stern Vollmer equation, whereas the Stern Vollmer plot for dtCoTP displayed a pronounced downward curvature (Figure 5). The efficiency of tCo quenching by Co^{2+} ions decreased in the order: dtC(o)TP > ss-DNA > ds-DNA, as evidenced by the reciprocal Stern Vollmer constants (Table 3).

Linear Stern Vollmer plots are consistent with both collisional and static quenching, although linearity alone does not prove the existence of either mechanism. However, linearity is indicative of the prevalence of a single quenching process. Combined static and collisional quenching usually results in an upward turn of the Stern Vollmer plot, while a downward turn indicates steric shielding and fractional accessibility of the fluor. In collisional quenching, the diffusive encounter between the fluor and the quencher lowers the energy of the excited state and the decay rate. Static quenching is the result of complex formation between the quencher and the fluor. Importantly, obtaining Stern Vollmer plots at different temperatures can distinguish between static and collisional quenching [51].

For all tCo species, we observed less efficient quenching at higher temperatures, which points toward a predominantly static quenching mechanism because higher temperatures typically aid the dissociation of molecular complexes. In contrast, high temperatures enhance dynamic quenching because it results in faster diffusion. The mere magnitude of K_{SV} also argues in favor of a static quenching mechanism. For dynamic quenching, the bimolecular quenching constant k_q can be calculated from the Stern Vollmer constant using $K_{SV} = k_q\tau_0$, with τ_0 being the lifetime of the unquenched fluor. With τ_0 = 5.6 ns for ss-tCo-

DNA [16] and $K_{SV} = 3500\ M^{-1}$, we obtain $k_q = 6 \times 10^{11}\ M^{-1}\ s^{-1}$, which is easily one order of magnitude larger than the maximal rate of diffusion controlled reactions in aqueous solution.

Due to different synthetic routes [15], only the free tC base, but not the tCo base was available for our studies. We therefore used the sulfur analogue tC to determine, if the basis for static quenching is binding of Co^{2+} ions to the negatively charged phosphate groups of DNA and nucleotides. When incorporated into DNA, tC and tCo behaved identically (table 3). However, the $(K_{SV})^{-1}$ for the free tC base was more than 1000-fold larger than for dtCTP, and the enhanced quenching at higher temperature confirms collisional quenching (Figure 5D). Thus, in the absence of phosphate groups, quenching is weak and mainly collisional while the presence of phosphates results in static quenching. This indicates that quenching of tC(o)TP and tC(o)-labeled DNA results from Co^{2+} binding to the phosphates of each species. This view is consistent with our observation of dequenching when Mg^{2+} ions are added to compete with Co^{2+} for the phosphate binding sites (Figure 5B). Similar to the effects of Co^{2+} on tCo in DNA, Atherton et al. reported quenching of DNA-intercalated ethidium bromide by phosphate-bound Co^{2+} ions [46].

Ethidium bromide was one of the first dyes used in real-time PCR [52]. Its fluorescence enhancement upon binding to double-stranded DNA is only 20-fold[53]. This is low compared to that of SybrGreenI (1000-fold)[54], which is today's gold standard for reporter-free real-time PCR. Since the Co^{2+} quenching constants for dtCoTP and tCo-labeled DNA differ by a factor of 20, the fluorescence contrast between free and incorporated tCo should easily be sufficient to observe DNA synthesis in real-time, provided the Co^{2+} concentration is kept low. However, the method would likely be inferior to using SybrGreen. The real strength of tCo may lie in the possibility to build molecular switches by placing tCo sites close to a specifically complexed Co^{2+} ion or by attaching the tCo to a locally phosphate-free nucleic acid backbone. Experiments to test this hypothesis are in progress.

CONCLUSION

In this publication, we explored the effect of Mn^{2+} and Co^{2+} ions on (a) the fluorescence emission of the base analogue tC(o) and (b) on the incorporation and replication of tC(o) by Taq polymerase. Mn^{2+} ions improved the catalytic efficiency for both correct and incorrect nucleotide insertion opposite and past a template tCo, resulting in significantly improved bypass of template tCo. Remarkably, Mn^{2+} improved the ability of Taq polymerase to distinguish between dtCoTP and dTTP, thus avoiding the polymerization of otherwise poorly extended dtCo-A mismatches. The altered polymerization kinetics in combination with the effects of betaine, a mild denaturation agent that is also a natural cofactor in DNA methylation, allowed for the synthesis of PCR fragments where ≥ 15% of the dC's were replaced by dtCo. Cobalt ions were shown to effectively quench tC(o) fluorescence through coordination of Co^{2+} to the phosphate groups of nucleic acids. Since tC(o) can be introduced to a specific site of the DNA strand, Co^{2+} quenching of the fluorescence may provide a powerful tool for probing the accessibility of the phosphate backbone of DNA in macromolecular complexes.

Acknowledgments

This work was supported by the NIH (GM093943 (B.P.), AI59764 (R.D.K) and GM073832 (R.D.K)) and the University of Denver (B.P).

References

1. Sinkeldam RW, et al. Fluorescent analogs of biomolecular building blocks: design, properties, and applications. Chem Rev. 2010; 110:2579–2619. [PubMed: 20205430]

2. Gondert ME, et al. Catalytic core structure of the trans-acting HDV ribozyme is subtly influenced by sequence variation outside the core. Biochemistry. 2006; 45:7563–7573. [PubMed: 16768452]
3. Seibert E, et al. Contribution of opening and bending dynamics to specific recognition of DNA damage. J Mol Biol. 2003; 330:687–703. [PubMed: 12850140]
4. Harris DA, et al. Local conformational changes in the catalytic core of the trans-acting hepatitis delta virus ribozyme accompany catalysis. Biochemistry. 2002; 41:12051–12061. [PubMed: 12356305]
5. Schlosser A, et al. Fluorescence-monitored conformational change on the 3'-end of tRNA upon aminoacylation. J Biomol Struct Dyn. 2001; 19:285–291. [PubMed: 11697733]
6. Walter NG, et al. A base change in the catalytic core of the hairpin ribozyme perturbs function but not domain docking. Biochemistry. 2001; 40:2580–2587. [PubMed: 11327881]
7. Lenz T, et al. 2-Aminopurine flipped into the active site of the adenine-specific DNA methyltransferase M.TaqI: crystal structures and time-resolved fluorescence. J Am Chem Soc. 2007; 129:6240–6248. [PubMed: 17455934]
8. Malta E, et al. Functions of base flipping in E. coli nucleotide excision repair. DNA Repair (Amst). 2008; 7:1647–1658. [PubMed: 18638572]
9. Szegedi SS, et al. Substrate binding in vitro and kinetics of RsrI [N6-adenine] DNA methyltransferase. Nucleic Acids Res. 2000; 28:3962–3971. [PubMed: 11024176]
10. Sastry SS, Ross BM. A direct real-time spectroscopic investigation of the mechanism of open complex formation by T7 RNA polymerase. Biochemistry. 1996; 35:15715–15725. [PubMed: 8961934]
11. Reha-Krantz LJ. The use of 2-aminopurine fluorescence to study DNA polymerase function. Methods Mol Biol. 2009; 521:381–396. [PubMed: 19563118]
12. Okamoto A, et al. Clear distinction of purine bases on the complementary strand by a fluorescence change of a novel fluorescent nucleoside. J Am Chem Soc. 2003; 125:4972–4973. [PubMed: 12708835]
13. Okamoto A, et al. Simple SNP typing assay using a base-discriminating fluorescent probe. Mol Biosyst. 2006; 2:122–127. [PubMed: 16880929]
14. Engman KC, et al. DNA adopts normal B-form upon incorporation of highly fluorescent DNA base analogue tC: NMR structure and UV-Vis spectroscopy characterization. Nucleic Acids Res. 2004; 32:5087–5095. [PubMed: 15452275]
15. Lin KY, J RJ, Matteucci MJ. Tricyclic 2'-deoxycytidine analogs—syntheses and incorporation into oligodeoxynucleotides which have enhanced binding to complementary RNA. J Am Chem Soc. 1995; 117:3873–3874.
16. Sandin P, et al. Characterization and use of an unprecedentedly bright and structurally non-perturbing fluorescent DNA base analogue. Nucleic Acids Res. 2008; 36:157–167. [PubMed: 18003656]
17. Stengel G, et al. Ambivalent incorporation of the fluorescent cytosine analogues tC and tCo by human DNA polymerase alpha and Klenow fragment. Biochemistry. 2009; 48:7547–7555. [PubMed: 19580325]
18. Stengel G, et al. High density labeling of polymerase chain reaction products with the fluorescent base analogue tCo. Anal Chem. 2009; 81:9079–9085. [PubMed: 19810708]
19. Stengel G, et al. Incorporation of the fluorescent ribonucleotide analogue tCTP by T7 RNA polymerase. Anal Chem. 2010; 82:1082–1089. [PubMed: 20067253]
20. Borjesson K, et al. Nucleic acid base analog FRET-pair facilitating detailed structural measurements in nucleic acid containing systems. J Am Chem Soc. 2009; 131:4288–4293. [PubMed: 19317504]
21. Stengel G, et al. Conformational dynamics of DNA polymerase probed with a novel fluorescent DNA base analogue. Biochemistry. 2007; 46:12289–12297. [PubMed: 17915941]
22. Beckman RA, et al. On the fidelity of DNA replication: manganese mutagenesis in vitro. Biochemistry. 1985; 24:5810–5817. [PubMed: 3910084]
23. Cadwell RC, Joyce GF. Mutagenic PCR. PCR Methods Appl. 1994; 3:S136–140. [PubMed: 7920233]

24. Michaels ML, et al. Evidence for in vitro translesion DNA synthesis past a site-specific aminofluorene adduct. J Biol Chem. 1987; 262:14648–14654. [PubMed: 3667596]
25. Tabor S, Richardson CC. Effect of manganese ions on the incorporation of dideoxynucleotides by bacteriophage T7 DNA polymerase and Escherichia coli DNA polymerase I. Proc Natl Acad Sci U S A. 1989; 86:4076–4080. [PubMed: 2657738]
26. Castro C, et al. Two proton transfers in the transition state for nucleotidyl transfer catalyzed by RNA- and DNA-dependent RNA and DNA polymerases. Proc Natl Acad Sci U S A. 2007; 104:4267–4272. [PubMed: 17360513]
27. Castro C, et al. Nucleic acid polymerases use a general acid for nucleotidyl transfer. Nat Struct Mol Biol. 2009; 16:212–218. [PubMed: 19151724]
28. Cisneros GA, et al. Catalytic mechanism of human DNA polymerase lambda with Mg2+ and Mn2+ from ab initio quantum mechanical/molecular mechanical studies. DNA Repair (Amst). 2008; 7:1824–1834. [PubMed: 18692600]
29. Steitz TA. A mechanism for all polymerases. Nature. 1998; 391:231–232. [PubMed: 9440683]
30. Li Y, et al. Crystal structures of open and closed forms of binary and ternary complexes of the large fragment of Thermus aquaticus DNA polymerase I: structural basis for nucleotide incorporation. Embo J. 1998; 17:7514–7525. [PubMed: 9857206]
31. Garcia-Diaz M, et al. Role of the catalytic metal during polymerization by DNA polymerase lambda. DNA Repair (Amst). 2007; 6:1333–1340. [PubMed: 17475573]
32. Frank EG, Woodgate R. Increased catalytic activity and altered fidelity of human DNA polymerase iota in the presence of manganese. J Biol Chem. 2007; 282:24689–24696. [PubMed: 17609217]
33. Hays H, Berdis AJ. Manganese substantially alters the dynamics of translesion DNA synthesis. Biochemistry. 2002; 41:4771–4778. [PubMed: 11939771]
34. Pence MG, et al. Lesion bypass of N2-ethylguanine by human DNA polymerase iota. J Biol Chem. 2009; 284:1732–1740. [PubMed: 18984581]
35. Villani G, et al. Effect of manganese on in vitro replication of damaged DNA catalyzed by the herpes simplex virus type-1 DNA polymerase. Nucleic Acids Res. 2002; 30:3323–3332. [PubMed: 12140316]
36. Voigt JM, Topal MD. O6-methylguanine-induced replication blocks. Carcinogenesis. 1995; 16:1775–1782. [PubMed: 7634403]
37. Blanca G, et al. Human DNA polymerase lambda diverged in evolution from DNA polymerase beta toward specific Mn(++) dependence: a kinetic and thermodynamic study. Biochemistry. 2003; 42:7467–7476. [PubMed: 12809503]
38. Ludwig J. A new route to nucleoside 5'-triphosphates. Acta Biochim Biophys Acad Sci Hung. 1981; 16:131–133. [PubMed: 7347985]
39. Fersht, A. Enzyme structure and mechanism. W.H. Freeman & Company; 1985.
40. Kunkel TA, Loeb LA. On the fidelity of DNA replication. Effect of divalent metal ion activators and deoxyrionucleoside triphosphate pools on in vitro mutagenesis. J Biol Chem. 1979; 254:5718–5725. [PubMed: 376517]
41. Morris SJ, et al. The use of cobalt ions as a collisional quencher to probe surface charge and stability of fluorescently labeled bilayer vesicles. Biochim Biophys Acta. 1985; 818:365–372. [PubMed: 4041444]
42. Holmes AS, et al. Fluorescence quenching by metal ions in lipid bilayers. Biophys Chem. 1993; 48:193–204. [PubMed: 8298057]
43. Sardar SK, et al. Interaction of ketocyanine dye with a Co2+ ion: an electronic spectroscopic study. J Phys Chem A. 2010; 114:10388–10394. [PubMed: 20828117]
44. Wang X, et al. A new fluorescent chemosensor detecting Co2+ and K+ in DMF buffered solution. J Fluoresc. 2010; 20:557–561. [PubMed: 20020318]
45. Rupcich N, et al. Quenching of fluorophore-labeled DNA oligonucleotides by divalent metal ions: implications for selection, design, and applications of signaling aptamers and signaling deoxyribozymes. J Am Chem Soc. 2006; 128:780–790. [PubMed: 16417367]
46. Atherton SJ, Beaumont PC. Quenching of the fluorescence of DNA-intercalated ethidium bromide by some transition netal ions. Journal of Physical Chemistry. 1986; 90:2252–2259.

47. Sarkar G, et al. Formamide can dramatically improve the specificity of PCR. Nucleic Acids Res. 1990; 18:7465. [PubMed: 2259646]

48. Varadaraj K, Skinner DM. Denaturants or cosolvents improve the specificity of PCR amplification of a G + C-rich DNA using genetically engineered DNA polymerases. Gene. 1994; 140:1–5. [PubMed: 8125324]

49. Baskaran N, et al. Uniform amplification of a mixture of deoxyribonucleic acids with varying GC content. Genome Res. 1996; 6:633–638. [PubMed: 8796351]

50. Weissensteiner T, Lanchbury JS. Strategy for controlling preferential amplification and avoiding false negatives in PCR typing. Biotechniques. 1996; 21:1102–1108. [PubMed: 8969839]

51. Lakowicz, JR. Principles of fluorescence spectroscopy. Springer; 2006.

52. Higuchi R, et al. Kinetic PCR analysis: real-time monitoring of DNA amplification reactions. Biotechnology (N Y). 1993; 11:1026–1030. [PubMed: 7764001]

53. Olmsted J 3rd, Kearns DR. Mechanism of ethidium bromide fluorescence enhancement on binding to nucleic acids. Biochemistry. 1977; 16:3647–3654. [PubMed: 889813]

54. Tuma RS, et al. Characterization of SYBR Gold nucleic acid gel stain: a dye optimized for use with 300-nm ultraviolet transilluminators. Anal Biochem. 1999; 268:278–288. [PubMed: 10075818]

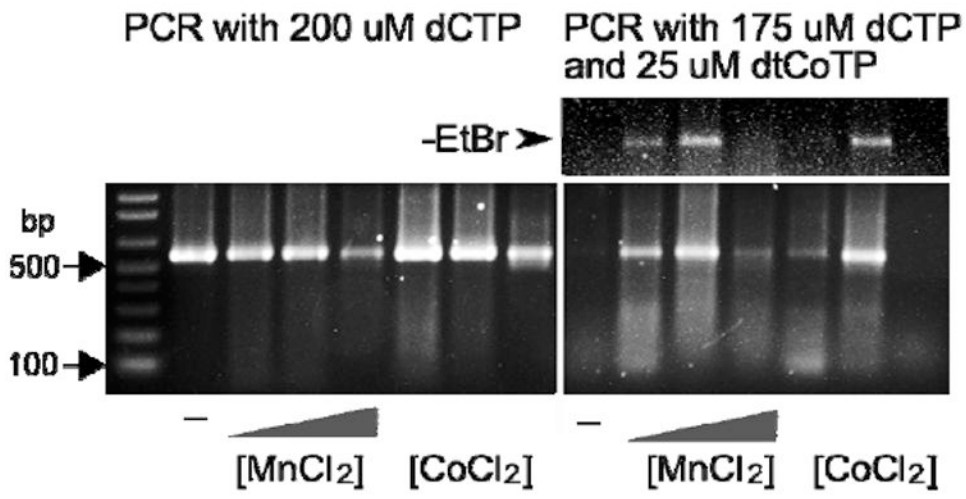

Figure 1.

Effect of Mn^{2+} or Co^{2+} ions on the PCR amplification of a 560 bp DNA fragment using Taq polymerase. The DNA was amplified in 30 cycles (94°C/45 s; 55°C/30 s; 72°C/2 min 30 s) using either the four natural nucleotides alone (left) or with added dtCoTP (right). All reactions contained 3.5 mM $MgCl_2$ and were supplemented with 0.2, 0.5 and 1 mM $MnCl_2$ or $CoCl_2$, respectively. PCR products were analyzed on a 1.2% agarose gel and visualized prior (top right) and after staining with ethidium bromide (EtBr).

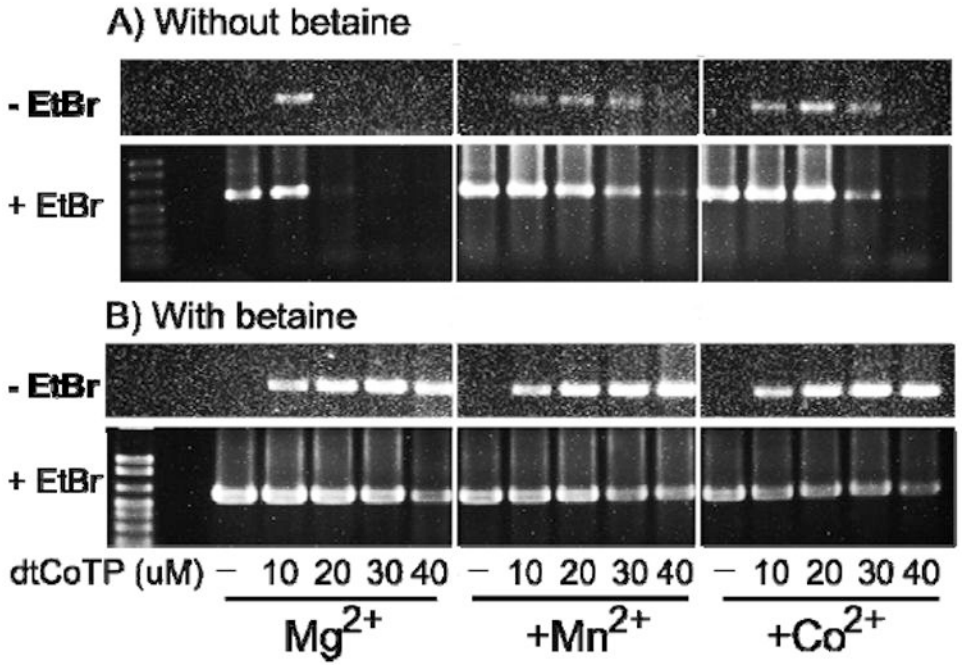

Figure 2.

Improvement of Taq pol catalyzed polymerase chain reactions by betaine and divalent ions. A) Reactions were performed without betaine (PCR settings: 30 cycles at 94°C/20 s; 55°C/30 s; 72°C/2 min 30 s). B) Reactions contained 1 M betaine (PCR settings: 30 cycles at 97°C/20 s; 55°C/30 s; 72°C/2 min 30 s). All reactions contained 200 μM of dGTP, dTTP, dATP and 3.5 mM $MgCl_2$. Where indicated $MnCl_2$ or $CoCl_2$ was added to a final concentration of 0.5 mM. Samples contained either only dCTP, or 10 μM, 20 μM, 30 μM dtCoTP and 40 μM dtCoTP, with [dtCoTP] + [dCTP] being 200 μM. Note that all PCR reactions were analyzed on the same agarose gel to make the intensities of the DNA bands comparable.

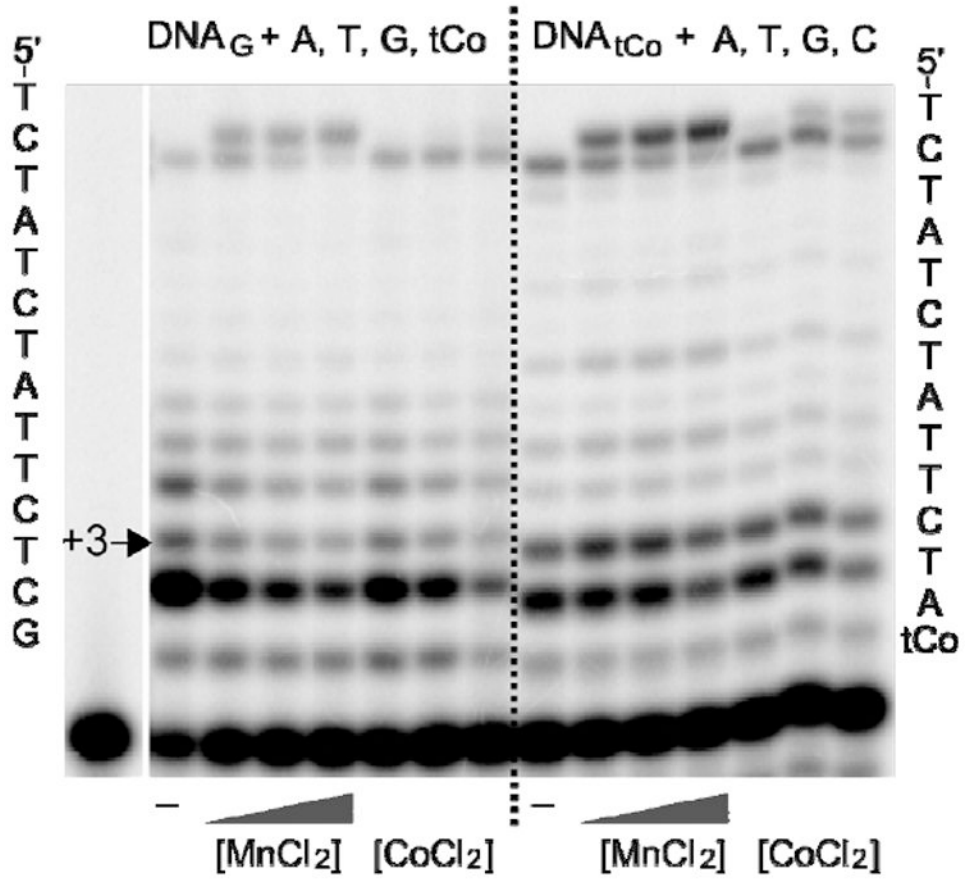

Figure 3.

Effect of varying concentrations of Mn^{2+} or Co^{2+} on the extension of synthetic primer/templates by Taq pol. The template sequences of DNA_G and DNA_{tCo} are shown left and right of the image, respectively. The very left lane is the no enzyme control. All reactions contained 0.05 units/μL Taq pol, 0.5 μM primer/template, 25 μM of the indicated dNTP, 3mM $MgCl_2$ and the indicated concentration of $MnCl_2$ or $CoCl_2$ (0.1, 0.2 or 0.5 mM). The reactions were stopped after 5 min, the products separated by denaturing PAGE and quantified using phosphor imagery (see table 1).

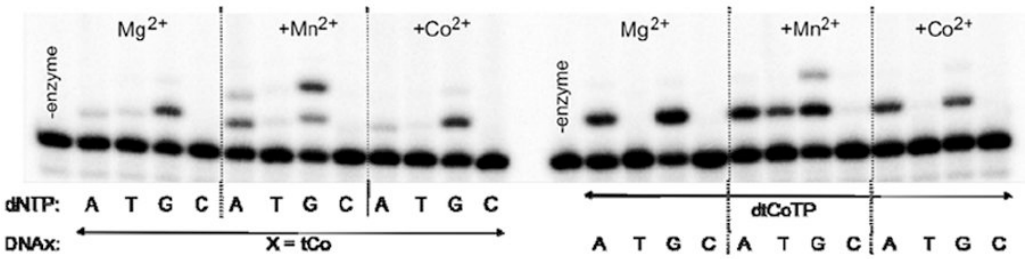

Figure 4.

Loss of specificity during single nucleotide incorporation in the presence of Mn2+ or Co2+ ions. The reactions containing 0.05 units/μL Taq pol, 0.5 μM of the indicated primer/template (DNA_X) and 25 μM of the indicated dNTP were allowed to proceed for 15 min. All reactions contained 3 mM $MgCl_2$, and 0.5 mM $MnCl_2$ or 0.5 mM $CoCl_2$, if indicated. The results of the detailed kinetic analysis of mismatch formation are shown in table 2.

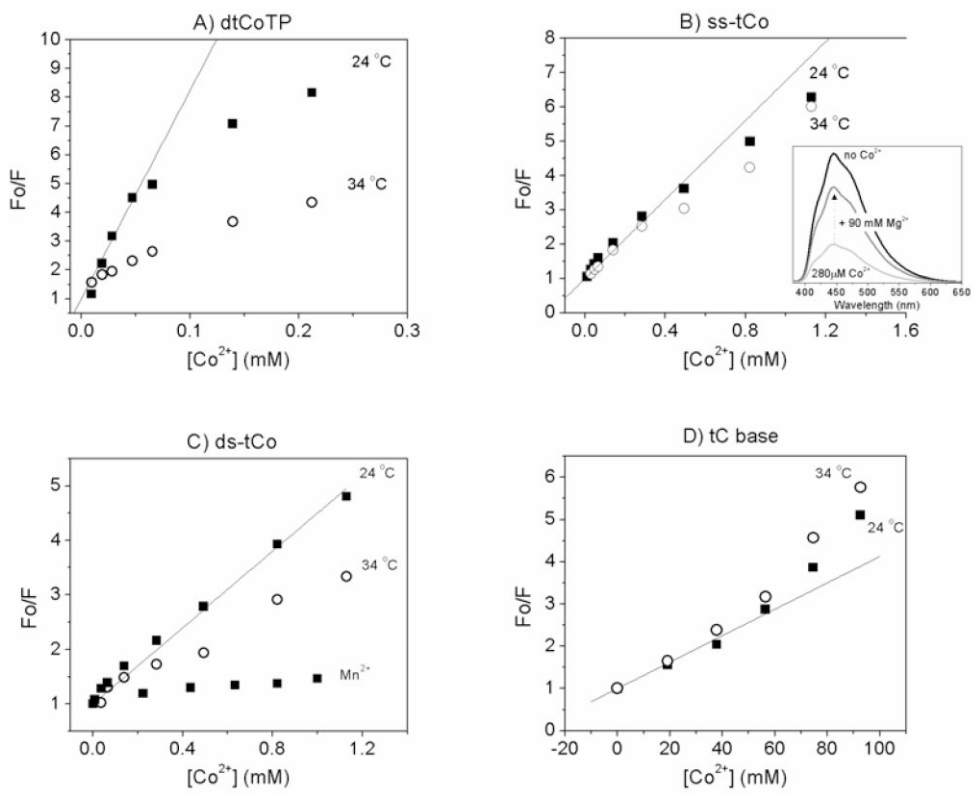

Figure 5.

Quenching of tC(o) fluorescence by Co^{2+} and Mn^{2+} ions. Solutions of dtCoTP (A), single-stranded oligonucleotide exhibiting one tCo (ss-tCo, B), its double-stranded complement (ds-tCo, C), or free tC base (D) were titrated with $CoCl_2$. Data points recorded at 24°C are displayed as black square, data points measured at 34°C as open circles. The inset of 5B shows the fluorescence emission spectra of ss-tCo without and with Co^{2+}, and after recovery of the tCo emission by addition of Mg^{2+}. The fluorescence intensity was measured before (F_0) and after (F) addition of quencher (Q) and are presented as Stern Vollmer plots, $F_0/F=1+K_{SV}[Q]$. The corresponding Stern Vollmer constants (K_{SV}) were obtained from the linear region of the plots and are listed in table 3.

Table 1

Effect of $MnCl_2$ or $CoCl_2$ on the extension of synthetic primer/templates by Taq pol (see figure 3).

	3 mM $MgCl_2$ plus						
		$MnCl_2$ (mM)			**$CoCl_2$ (mM)**		
		0.1	**0.2**	**0.5**	**0.1**	**0.2**	**0.5**
DNA_G + dATP, dTTP, dGTP, dtCoTP							
Total extension (%)	75	44	33	27	42	28	19
Extension past +3 position (%)	64	72	72	75	64	67	69
DNA_{tCo} + dATP, dTTP, dGTP, dCTP							
Total extension (%)	27	36	37	31	27	26	17
Extension past +3 position (%)	48	52	56	66	48	52	57

Anal Biochem. Author manuscript; available in PMC 2012 September 1.

Table 2

Comparison of kinetic parameters for mismatch insertion with Mg2+ and Mn2+ ions as cofactors.

Template	Incoming dNTP	Metal ion	K_M[#] (μM)	V_{max}[#] (% min^{-1})	V_{max}/K_M (% μM^{-1} min^{-1})	$\frac{(V_{max}/K_M)_{Mn2+}}{(V_{max}/K_M)_{Mg2+}}$
Kinetic parameters for single nucleotide incorporations at the +1 template position						
DNA-tCo	dGTP	Mn^{2+}	1.4 (0.2)	3.4 (0.1)	2.4	3
DNA-tCo	dGTP	Mg^{2+}	12 (3)	10 (1)	0.8[*]	
DNA-tCo	dATP	Mn^{2+}	7.9 (0.9)	1.9 (0.1)	0.2	7
DNA-tCo	dATP	Mg^{2+}	20 (4)	0.58 (0.03)	0.03[*]	
DNA-C	dGTP	Mn^{2+}	0.17 (0.02)	14.5 (0.3)	86	2
DNA-C	dGTP	Mg^{2+}	0.44 (0.05)	16.5 (0.6)	38	
DNA-C	dATP	Mn^{2+}	22 (6)	1.7 (0.2)	0.1	>2000
DNA-C	dATP	Mg^{2+}			< 0.00005[$]	
Kinetic parameters for single nucleotide incorporations at the +3 template position						
DNA-tCo	dATP	Mn^{2+}	1.1 (0.1)	0.14 (0.01)	0.1	10
DNA-tCo	dATP	Mg^{2+}	6 (1)	0.07 (0.01)	0.01	
DNA-C	dATP	Mn^{2+}	0.19 (0.03)	0.51 (0.01)	2.7	13
DNA-C	dATP	Mg^{2+}	1.8 (0.3)	0.38 (0.02)	0.2	
Kinetic parameters for competitive nucleotide incorporations at the +1 template position						
Template	**Competing dNTPs**	**Metal ion**	$(k_{cat}/K_M)_{dtCoTP}/(k_{cat}/K_M)_{correct\ dNTP}$			
DNA-G	dtCoTP/dCTP	Mn^{2+}	2			0.3
DNA-G	dtCoTP/dCTP	Mg^{2+}	7.7[*]			
DNA-A	dtCoTP/dTTP	Mn^{2+}	0.03			0.1
DNA-A	dtCoTP/dTTP	Mg^{2+}	0.3[*]			

[*] Previously published in reference 4.

[#] Errors are provided in brackets.

[$] n. d. less than 2% incorporation after 40 min at 1mM dNTP

All reactions contained 3 mM $MgCl_2$ and 0.5 mM $MnCl_2$ if indicated.

Table 3

Stern Vollmer constants for quenching of tricyclic cytosines.

	Reciprocal Stern Vollmer Constant* $(K_{SV})^{-1}$ (μM)
dtCoTP	14
ss-tCo	174
ds-tCo	285
ds-tCo (quenching by Mn^{2+})	19,880
tC base	32,000
dtCTP	12
ss-tC	118
ds-tC	153

*quenching by Co^{2+} in 20 mM Tris/HCl pH8, 50 mM NaCl at 24°C.